

# Initial Applications of Synchrophasors Using Area Angles

by

Hussam Schwail

A thesis submitted in partial fulfillment of  
the requirements for the degree of

Master of Science  
(Electrical Engineering)

at the

UNIVERSITY OF WISCONSIN-MADISON  
2012

© Copyright by Hussam Sehwal, 2012  
All Rights Reserved

## Acknowledgments

First, I must give thanks and praise to Allah, glorified and exalted is He, for all the favors and opportunities bestowed upon me in life. I thank Him for allowing me the privilege of attending fine institutions of learning. He has sustained me with provision, allowing me to approach the end of six years of college without any financial debt. My affairs have been made easy by Him. There were so many times when it seemed difficult or even impossible to resolve a situation, yet He granted me the means to success. Most of all, I am grateful for all guidance and wisdom He has blessed me with. I hope He leads me to be a means of benefit to others and contribute good to the world.

Next, I wish to express my deep gratitude to my advisor, Professor Ian Dobson. He brought me into the field of research I had been hoping to enter, allowing me to take part in fascinating work regarding real problems. His dexterity and experience permitted us to readdress the many roadblocks I presented to him during our work. Though my mind may not be nearly as deep or sophisticated as his, I hope that some of his intelligence has seeped through to me. Most of all, I am grateful for the way he treated me. He has always been kind, encouraged me to explore, and shown respect to my thoughts and suggestions. I hope our work together has been as valuable to him as it has been to me and that we can find ways to work together in the future.

Then, of course, is my profound appreciation to my family. I know my parents made great efforts and sacrifices not just for our family in general, but even for me in particular. Though they had limited means, my parents strove throughout my life so that I may receive a proper education. I know I can appear very studious and serious, spending little time with them during my college studies. Nonetheless, they have continued to support and encourage me. I pray they forgive me for my shortcomings as a son and that they are happy with my achievements. I would also like to thank my siblings who have been an outlet for my joy during the successes of my career. And I am especially grateful to my brother Walaid who, despite our differences, has continued to express pride in my accomplishments and found it in him to speak highly of me.

My thanks to the university for the wonderful education it has provided and I hope it continues to do so for many others. I would also like to recognize the funders. This work was coordinated by the Consortium for Electric Reliability Technology Solutions with funding provided in part by the California Energy Commission Public Interest Energy Research Program, under Work for Others Contract No. 500-08-054. The Lawrence Berkeley National Laboratory is operated under DOE Contract No. DE-AC02-05CH11231. Funding from graduate school at the University of Wisconsin is gratefully acknowledged.

Finally, I would like to express gratitude to my friends, my teachers, and all those who supported me throughout the way.

Hussam Schwail  
May 15, 2012  
Madison, Wisconsin

# Table of Contents

<b>Acknowledgments</b>	<b>i</b>
<b>Table of Contents</b>	<b>ii</b>
<b>List of Tables</b>	<b>iv</b>
<b>List of Figures</b>	<b>v</b>
<b>Abstract</b>	<b>vi</b>
<b>1 Introduction</b>	<b>1</b>
<b>2 Applying synchrophasor computations to a specific area</b>	<b>3</b>
2.1 Area decoupling by superposition . . . . .	3
2.2 Measurements to get area internal angles . . . . .	5
2.3 Tate and Overbye's method of line outage detection . . . . .	6
2.4 Example: applying Tate and Overbye's method to an area . . . . .	7
2.5 Conclusion . . . . .	8
<b>3 Locating line outages in a specific area of a power system with syn-</b> <b>chrophasors</b>	<b>10</b>
3.1 Introduction . . . . .	10
3.2 Review of Tate and Overbye's method . . . . .	11
3.3 Reduction to specified area . . . . .	15
3.3.1 Non-islanding outage . . . . .	18
3.3.2 Islanding outage . . . . .	19
Line outage modeling . . . . .	20

Redispatch . . . . .	23
Island referencing . . . . .	24
3.3.3 Example . . . . .	25
3.4 Conclusions . . . . .	27
<b>4 Examples of voltages across areas in WECC</b>	<b>29</b>
4.0.1 Angle across an area . . . . .	29
4.0.2 Simple example . . . . .	30
4.1 Southern California area . . . . .	31
4.1.1 Methodology overview . . . . .	31
4.1.2 Results . . . . .	34
4.2 Areas North and South of COI . . . . .	40
4.2.1 Area North of COI . . . . .	40
4.2.2 Area South of COI . . . . .	43
<b>Bibliography</b>	<b>46</b>

# List of Tables

2.1	Area angles . . . . .	8
3.1	Predicted Outage According to synchrophasor Buses . . . . .	26
4.1	Area 1 (in degrees) . . . . .	36
	(a) Subtable 1a . . . . .	36
	(b) Subtable 1b . . . . .	36
4.2	Area 2 (in degrees) . . . . .	36
	(a) Subtable 2a . . . . .	36
	(b) Subtable 2b . . . . .	36
4.3	Area 3 (in degrees) . . . . .	37
	(a) Subtable 3a . . . . .	37
	(b) Subtable 3b . . . . .	37
4.4	Area 4 (in degrees) . . . . .	37
	(a) Subtable 4a . . . . .	37
	(b) Subtable 4b . . . . .	37
4.5	Percent Changes in $\hat{\theta}_A$ . . . . .	38
4.6	Border bus weighting in North of COI area angle . . . . .	42
4.7	Border bus weighting in South of COI area angle . . . . .	43

## List of Figures

2.1	An area R consisting of buses with thicker circles or squares 4, 5, 6, 7, 8, 10, 11, 12, 13, 14, 31, 32 in the 39 bus New England test system. Border buses 4, 8, 14 are shown with squares. . . . .	7
3.1	Reduced New England System Model . . . . .	25
4.1	A power system area to show the angle across the area from buses 31, 32 to buses 39,4,14. The area angle can be thought of as the angle across the single transmission line a-b shown that is a reduced equivalent of the area.	31
4.2	WECC model . . . . .	33
4.3	Southern California areas. Area border buses are shown as triangles. . . . .	35
	(a) Area 1 . . . . .	35
	(b) Area 2 . . . . .	35
	(c) Area 3 . . . . .	35
	(d) Area 4 . . . . .	35
4.4	North of COI area electric network . . . . .	41
4.5	South of COI area electric network . . . . .	44

## Abstract

Synchrophasors allow fast, synchronized measurements of the power grid and have the potential to serve power system applications more effectively. Synchrophasor data may allow analyzing subareas of the system without need for access to outer area information. This thesis focuses on implementing the area angle concept on subareas of networks for various power system tasks. First, we show the ability to decouple a subnetwork using only the area's synchrophasor measurements and superposition. Next we present a line outage detection algorithm within an area for both islanding and non-islanding cases. Finally, we discuss defining area angles for meaningful analysis of a power system, particularly for areas in the WECC system.



# Chapter 1

## Introduction

The development of phasor measurement unit (PMU) technology presents new possibilities for the power grid and challenges for research. The PMU technology gives fast, synchronized measurements coordinated over the entire power system. Faster data allows more effective analysis of power systems and could significantly improve operation. However, the ways in which PMU data can be used to achieve this are still being established. PMU measurements can be used to detect and record events over the entire power grid, calibrate dynamic models, detect and quantify slow oscillations, and augment state estimation [1].

There have been studies showing that the phase angle difference between two buses can be used to give a measure of the stress between the buses [2]. Such measurements, however, are generally affected by changes across the entire system and may not give indications of changes in the state of the system that are easy to interpret.

This thesis focusses on applying PMU measurements that are in a particular area or subnetwork of the grid. The effects of the rest of the grid are taken into account by PMU measurements at all the tie lines around the border of the area, but the algorithms to process the measurements can work with only a model of the area. The motivation is that utilities and other organizations are commonly responsible for only one area of the power system and they have better access to information about their own area and the computations can be more practical for an area rather than the entire interconnected power system. Many of the opportunities for advanced applications of PMU measurements involve both the measurements and power system models.

The new concept of angles across areas of power systems [3] presents another potential tool for utilizing PMU data for power system monitoring and control. The area angle

is a metric of stress across a specifically defined area and may enable several practical applications in the near future. An area of the system is determined by a choice of border buses at all the tie lines to the area. The area is reduced to an equivalent area made only of border buses so as to then combine weighted bus angles to produce a measure of the angle across the area. There has also been discussion of combining phasor voltage angles by weighting bus angles based on the sensitivity of each bus [4].

This thesis focuses on the implementation of the area angles and related area concepts in power systems to monitor and detect line outages and associated changes in stress across areas. The approach is mainly through developing algorithms based on the area equations and analyzing computer models of power systems.

It is advantageous to adapt power grid algorithms using PMU measurements so that they can work on power system areas. Chapter 2 discusses implementing the area angle concept where only an area (subnetwork) of a system is observable. This chapter illustrates how to process PMU measurements in such an area by in effect decoupling it from the rest of the system using border measurements. The processed measurements can be used to determine if phasor angle changes are due to line outages inside the area or not.

Chapter 3 presents an algorithm adapting a line-outage prediction algorithm developed by Tate and Overbye [5] for an entire network to work in an area of the power system. The method uses only the PMU measurements inside the area. The algorithm also furthers the previous work by allowing the prediction of line outages which disconnect the system into separate islands.

Finally Chapter 4 defines areas for analyzing area stress in a fairly detailed model of the WECC Western grid interconnection. A simulation of events for the San Diego blackout of September 2011 is used for exploring the changes in stress as the outages proceed.

## Chapter 2

# Applying synchrophasor computations to a specific area

There are good opportunities for calculations that combine synchrophasor measurements with power system models. However, in large interconnections, it is often convenient for utilities to maintain network models only for their own area. Using superposition, calculations using models and synchrophasor measurements at all the border buses of an area of a power system can be used to effectively decouple the area from the rest of the power system. We illustrate the decoupling for a line outage detection algorithm.

### 2.1 Area decoupling by superposition

We denote the area of interest by  $R$ , and first account for the effect of the rest of the network on  $R$  by a vector of power injections  $P_r^{\text{into}}$  into  $R$  at all the border buses of  $R$  that have tie lines connecting  $R$  to the rest of the network. For each border bus of  $R$ , the corresponding entry of the vector  $P_r^{\text{into}}$  is the sum of real power flows of the tie lines that are incident on that border bus. For each interior bus of  $R$ , the corresponding entry of the vector  $P_r^{\text{into}}$  is zero. We write  $P_r^R$  for the real power injections (generation or load) at buses inside  $R$ . Then the total power injections at area buses are  $P_r^R + P_r^{\text{into}}$ . Write  $\theta_r$  for the voltage angles at buses inside  $R$ , and  $B_{rr}^R$  for the susceptance matrix of area  $R$  considered as a stand-alone network. Then the DC load flow for area  $R$  is

$$B_{rr}^R \theta_r = P_r^R + P_r^{\text{into}} \quad (2.1)$$

Let  $\theta_r^{\text{into}}$  be the part of the angles corresponding to the tie line power flows so that

$$P_r^{\text{into}} = B_{rr}^{\text{R}} \theta_r^{\text{into}} \quad (2.2)$$

Let  $\theta_r^{\text{R}}$  be the part of the angles corresponding to the power injections inside R so that  $P_r^{\text{R}} = B_{rr}^{\text{R}} \theta_r^{\text{R}}$ . We call  $\theta_r^{\text{R}}$  the *internal* voltage angles for area R. We use a common angle reference for all angles. Then

$$\theta_r = \theta_r^{\text{into}} + \theta_r^{\text{R}} \quad (2.3)$$

To summarize, superposition enabled by the linearity of the DC load flow implies that area R angles  $\theta_r$  are the sum of internal angles  $\theta_r^{\text{R}}$  due to the power injections inside R and angles  $\theta_r^{\text{into}}$  due to the power flows into R along the tie lines. Then (2.1) may be rewritten as

$$P_r^{\text{R}} = B_{rr}^{\text{R}} (\theta_r - \theta_r^{\text{into}}) = B_{rr}^{\text{R}} \theta_r^{\text{R}} \quad (2.4)$$

The internal angles  $\theta_r^{\text{R}} = \theta_r - \theta_r^{\text{into}}$  are obtained by adjusting the area angles  $\theta_r$  by subtracting  $\theta_r^{\text{into}}$ . Equation (2.4) shows that the internal angles  $\theta_r^{\text{R}}$  satisfy the DC load flow equation of the area R as if area R were a stand-alone area separated from the rest of the network.

An alternative derivation of (2.4) starts from the DC load flow of the entire network. Write  $\theta_{\bar{r}}$  and  $P_{\bar{r}}$  respectively for the voltage angles and real power injections at buses outside R. Order the buses so that the area buses R are first. Then the DC load flow

$P = B\theta$  for the entire network is

$$\begin{pmatrix} P_r^R \\ P_{\bar{r}} \end{pmatrix} = \begin{pmatrix} B_{rr} & B_{r\bar{r}} \\ B_{\bar{r}r} & B_{\bar{r}\bar{r}} \end{pmatrix} \begin{pmatrix} \theta_r \\ \theta_{\bar{r}} \end{pmatrix}. \quad (2.5)$$

The powers flowing into R along the tie lines are

$$P_r^{\text{into}} = \sum_{j \in \bar{r}} (-B_{rj})(\theta_j - \theta_r) = -B_{r\bar{r}}\theta_{\bar{r}} + \text{diag}\{B_{r\bar{r}}\mathbf{1}\}\theta_r$$

Here  $\mathbf{1}$  is a column vector of all ones. The first block row of (2.5) may be rewritten as

$$P_r^R = B_{rr}^R \theta_r - P_r^{\text{into}} \quad (2.6)$$

where  $B_{rr}^R = B_{rr} + \text{diag}\{B_{r\bar{r}}\mathbf{1}\}$  is the susceptance matrix for the area R considered as a stand-alone network. ( $B_{rr}^R$  is different than the submatrix  $B_{rr}$  of the susceptance matrix for the entire network, because the diagonal entries of  $B_{rr}^R$  do not include the tie line susceptances.) Then (2.2) can be used to rewrite (2.6) as (2.4).

## 2.2 Measurements to get area internal angles

We suppose that the following are available:

- Synchrophasor measurements  $\theta_s$  of voltage angles at some buses inside area R ( $\theta_s$  is a vector that is some of the components of  $\theta_r$ ).
- Synchrophasor measurements of the entering currents and voltages at all the tie lines joining to area R buses. This yields the powers  $P_r^{\text{into}}$  entering the border buses of R along all the tie lines.
- Area susceptance matrix  $B_{rr}^R$ . This is easily calculated from the current topology [5].

Then the internal voltage phasor angles  $\theta_s^R$  at the buses measured with synchrophasors can be computed as follows:

1. Obtain  $\theta_r^{\text{into}}$  from (2.2).  $\theta_s^{\text{into}}$  is some components of  $\theta_r^{\text{into}}$ .
2. Obtain internal angles  $\theta_s^R$  using  $\theta_s^R = \theta_s - \theta_s^{\text{into}}$ . This equation corresponds to some of the components of (2.3).

### 2.3 Tate and Overbye's method of line outage detection

It is useful to detect and locate transmission line outages with synchrophasor measurements. The information can confirm topology changes available from the traditional, slower SCADA and state estimation methods and provide the fast topology updates needed for other synchrophasor applications. Tate and Overbye [5] describe a method to detect and locate line outages in an entire network interconnection using synchrophasor measurements and a DC load flow model of the entire network. They model the effect of a line outage by a change  $\Delta P$  in power injections that consists of equal and opposite power injections at the ends of the line. The change in bus voltage angles  $\Delta\theta$  corresponding to the line outage is computed from the DC load flow

$$\Delta P = B\Delta\theta \tag{2.7}$$

The effect of each line outage on  $\Delta\theta$  is computed at the synchrophasor buses, and compared to the observed changes in synchrophasor voltage angle measurements. The line that outaged is identified as the line with the computed effect closest to that observed. Applying Tate and Overbye's method to a large interconnection requires maintaining a large DC load flow model and discriminating among many possible line outages, so here we show how to simply adapt the method to a given area within the interconnection.

## 2.4 Example: applying Tate and Overbye's method to an area

Fig. 2.1 shows an example of an area R in the 39 bus New England test system (network data are given in [3]). Bus 32 serves as the reference bus. There are synchrophasor voltage measurements at area border buses 4,8,14 and at buses 12,32 inside the area. There are synchrophasor measurements of the currents in the area tie lines 8–9, 4–3, 14–15. Assume that a change in voltage angles is detected, and that differences in the measurements before and after the change are obtained [5]. In particular, the change in the measured voltage angles  $\Delta\theta_s$  and the change in the tie line powers  $\Delta P_r^{\text{into}}$  can be obtained. The corresponding change  $\Delta\theta_r^{\text{into}}$  in area angles can be calculated using  $\Delta P_r^{\text{into}} = B_{rr}^R \Delta\theta_r^{\text{into}}$ . The changes in the internal voltage angles at the measured buses are computed using  $\Delta\theta_s^R = \Delta\theta_s - \Delta\theta_s^{\text{into}}$ . Then Tate and Overbye's method compares the internal angle changes  $\Delta\theta_s^R$  from measurements with the internal angle changes for

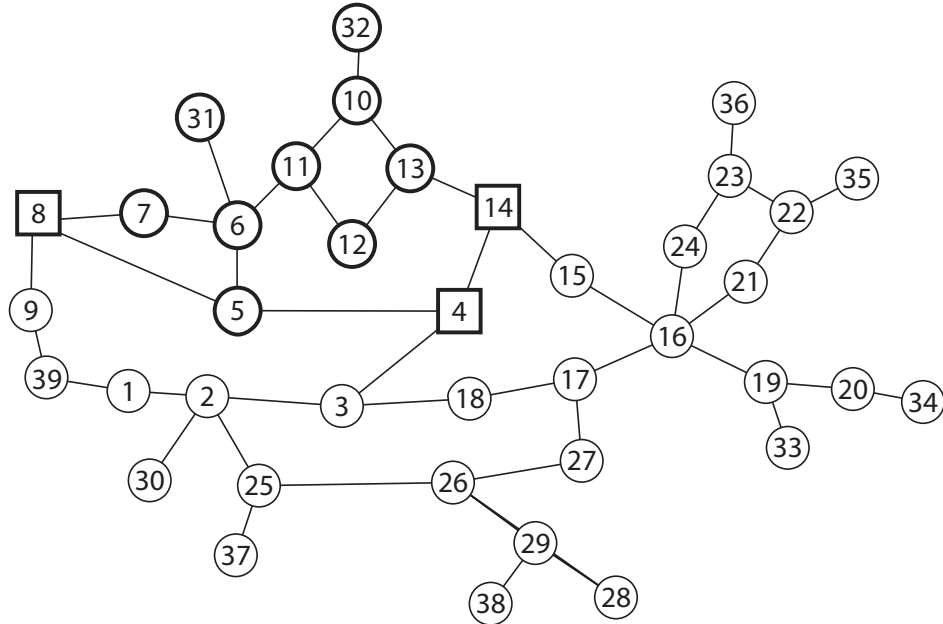


Figure 2.1: An area R consisting of buses with thicker circles or squares 4, 5, 6, 7, 8, 10, 11, 12, 13, 14, 31, 32 in the 39 bus New England test system. Border buses 4, 8, 14 are shown with squares.

each line computed using for (2.7) the incremental version of (2.4):

$$\Delta P_r^R = B_{rr}^R \Delta \theta_r^R \quad (2.8)$$

Table 2.1 shows how the base case angles  $\theta_s$  at synchrophasor buses split into internal angles  $\theta_s^R$  and angles  $\theta_s^{\text{into}}$  due to the tie line flows. A line outage inside the area such as 10-11 causes changes in internal angles that can be used in Tate and Overbye's method. Table 2.1 also shows that a line outage outside area R such as 2-3 leads to changes in area angles  $\theta_s$ , but the internal angles  $\theta_s^R$  do not change. In general, line outages or power redispatches outside the area do not affect the area power injections  $P_r$  and therefore, according to (2.4), the internal angles  $\theta_s^R$  do not change. Thus changes or not in internal angles can be used to detect whether the line outage occurs inside the area or not.

bus	base case			line 10-11 out		line 2-3 out	
	$\theta_s$	$\theta_s^{\text{into}}$	$\theta_s^R$	$\Delta \theta_s$	$\Delta \theta_s^R$	$\Delta \theta_s$	$\Delta \theta_s^R$
4	-11.68	0.37	-12.23	-3.62	-3.68	-0.59	0
8	-12.66	0.21	-12.87	-5.21	-5.40	0.63	0
12	-8.35	0.01	-8.36	-3.70	-3.70	0	0
14	-9.91	0.06	-9.98	-2.20	-2.07	-0.23	0
32	0	0	0	0	0	0	0

all angles in degrees

Table 2.1: Area angles

## 2.5 Conclusion

We show how to compute from synchrophasor measurements internal voltage angles that only respond to changes inside the area and correspond to models of the area that are effectively decoupled from the rest of the network. We illustrate the use of the internal voltage angles by applying Tate and Overbye's line outage algorithm to an area. The



method will be particularly useful when utilities or ISOs in large interconnections restrict their attention to network models and phasor measurements for only their own area. The results show the value of making phasor measurements at all the tie lines of an area. According to [3], phasor measurements at all the tie lines also enable area stress angles to be calculated.

Our example of the decoupling uses voltage angles and a DC power flow. However, since the decoupling depends only on linear circuit laws, we emphasize that exactly similar results apply to complex voltages and currents in an AC load flow model [3]. That is, we can compute from synchrophasor measurements internal complex voltages  $V_r^R = V_r - V_r^{\text{into}}$ , where  $V_r^{\text{into}}$  correspond to complex current injections  $I_r^{\text{into}}$  along the area ties lines according to  $I_r^{\text{into}} = Y_{rr} V_r^{\text{into}}$ , where  $Y_{rr}$  is the complex admittance matrix of the area.

## Chapter 3

# Locating line outages in a specific area of a power system with synchrophasors

We detect the location of line outages inside a specific area of the power system from synchrophasor measurements at the border of the area and inside the area. We process the area synchrophasor measurements using a DC load flow model of the area. The processed measurements do not respond to line trips or power redispatches outside the area. The method extends previous methods that locate line trips in an entire network so that they work in a particular area and also deals with cases of islanding. The method will be particularly useful when utilities or ISOs in large interconnections restrict their attention to network models and phasor measurements for only their own area.

### 3.1 Introduction

It is useful to detect and locate transmission line outages with synchrophasor measurements. The information can confirm topology changes available from the traditional, slower SCADA and state estimation methods and provide fast topology updates needed for other synchrophasor applications.

Tate and Overbye [5] give a method of detecting and locating line outages in an entire network interconnection by processing synchrophasor observations in an entire power grid. Edge detection methods are applied to detect changes in synchrophasor angles that exceed a threshold. The synchrophasor measurements are filtered to retain the changes in the steady state angle but suppress the settling transient that follows the line outage. Once a change in synchrophasor angles is detected and calculated, Tate and Overbye then give an algorithm to locate the line outage by comparing the observed

change in angles to the changes in angle for all the possible line outages computed using a DC load flow model of the entire network.

For this paper, we assume that changes in synchrophasor angles are available using the detection and filtering methods in Tate and Overbye [5], and show how to adapt their line outage location method to an area within the interconnection with synchrophasor measurements inside the area and around the border of the area. The border measurements are used to decouple the area from the rest of the network so that the method detects whether the line outage occurs within the area and then locates a line outage within the area using a DC load flow model of the area. The motivation is that it is often convenient for utilities to maintain network models only for their own area, and line outage detection algorithms can work better if there are fewer candidate line outage to choose from. Our approach also confirms whether the line outage occurred inside the monitored area or not, giving a useful discrimination of the source of changes in the power system.

Line outage detection is more complicated in cases in which the line outage islands the system because the rebalancing of generation in the areas needs to be taken into account. We extend Tate and Overbye’s method to accommodate islanding.

This paper begins with a review of the method established by Tate and Overbye, then discusses implementing the algorithm to a reduced area of the network for both non-islanding and islanding cases, and finishes with a simple example illustrating the concepts of the method.

### **3.2 Review of Tate and Overbye’s method**

We review Tate and Overbye’s method [5] of using observed changes in synchrophasor measurements to estimate the most likely line outages. The method is based on the DC load flow model, and

$$B\Delta\theta = \Delta P, \quad (3.1)$$

where  $\Delta P$  is a vector of the change in real power injection at each bus after the line outage,  $B$  is the susceptance matrix, and  $\Delta\theta$  is a vector of the changes in voltage phasor angle at each bus after the line outage. We note that in the DC load flow model, a line outage can be simulated as equal, but opposite power injections at the ends of the line so long as the system stays connected after the line outage [6]. (Modeling the line outage as power injections in a network with unchanged lines avoids the inconvenient recalculation of the susceptance matrix with the line removed.) Following a line outage, a change in the phasor angles is expected. A vector proportional to this change in angles is calculated for every possible line outage and compared to the observed change in angles. Since the synchrophasors are only at some of the buses, only some of the angle changes are known. The vector of the observed bus angles is  $\theta_{obs}$  and the vector of calculated (predicted) angles is  $\theta_{calc}$ . To relate the observed bus angles to all the buses, we introduce the matrix

$$K = [I_{M \times M} \quad \mathbf{0}_{M \times (N-M)}] \quad (3.2)$$

where  $N$  is the number of buses in the system and  $M$  is the number of buses observed with synchrophasors. Then

$$\theta_{obs} = K\theta \quad (3.3)$$

Since a line outage can be modeled by equal and opposite power injections at the buses at each end of the line [5], the form of  $\Delta P$  for the outage of a line  $l$  is<sup>1</sup>

$$\Delta P_{calc,l} = \begin{bmatrix} \mathbf{0} \\ \tilde{P}_l \\ \mathbf{0} \\ -\tilde{P}_l \\ \mathbf{0} \end{bmatrix} \begin{array}{l} \leftarrow \text{start bus} \\ \\ \\ \leftarrow \text{end bus} \end{array} . \quad (3.4)$$

The power injection  $\tilde{P}_l$  is related to the pre-outage flow  $P_l$  on line  $l$  according to

$$\tilde{P}_l = \frac{-P_l}{1 + \text{PTDF}_{l,l_{to}-l_{from}}} . \quad (3.5)$$

$\text{PTDF}_{l,l_{to}-l_{from}}$  is the power transfer distribution factor giving the increment in real power on the line when 1 MW is injected at the “to” bus of line  $l$  and  $-1$  MW is injected at the “from” bus of line  $l$ . It can be shown [6] that the injections  $\tilde{P}_l$  make the powers entering the “to” bus from lines other than line  $l$  sum to zero and the powers entering the “from” bus from lines other than line  $l$  sum to zero, and hence have the same effect as removing line  $l$ . We will see that the following calculation does not depend on the value of  $\tilde{P}_l$  or the value of  $P_l$ .

---

<sup>1</sup> $\mathbf{0}$  is a column vector of all zeros with the number of components chosen to fit the context.

We now calculate based on (3.1) the change in the angle  $\theta_{calc,l}$  for the outage of line  $l$

$$\begin{aligned}
\Delta\theta_{calc,l} &= KB^{-1}\Delta P_{calc,l} \\
&= \tilde{P}_l KB^{-1} \begin{bmatrix} \mathbf{0} \\ 1 \\ \mathbf{0} \\ -1 \\ \mathbf{0} \end{bmatrix} \\
&= \tilde{P}_l \Delta\tilde{\theta}_{calc,l}
\end{aligned} \tag{3.6}$$

Here it is convenient to write  $B^{-1}\Delta P_{calc,l}$  for the solution  $\Delta\theta$  to  $\Delta P_{calc,l} = B\Delta\theta$ . One approach is to solve  $\Delta P_{calc,l} = B\Delta\theta$  using the generalized inverse of matrix  $B$  [7]. We do not need to calculate the constant  $P_l$  as we can compare versions of  $\Delta\theta_{obs}$  and  $\Delta\tilde{\theta}_{calc,l}$  that are normalized to unit length. That is, we compare  $\widehat{\Delta\theta}_{obs}$  and  $\widehat{\Delta\tilde{\theta}}_{calc,l}$ , where  $\hat{x} = x/\|x\|$ . This implies that we do not need to know the actual power flows on the line nor the actual power injections representing the line outage that are in our predictions, because only the system's structure will determine the vector shape. We seek to compute the magnitude of error between the shapes of the calculated and observed vectors. This corresponds to the least geometric distance in the vector space of angle changes called the Normalized Angle Distance (NAD). The NAD between vectors of angle changes  $a$

and  $b$  has the following definition<sup>2</sup>:

$$\text{NAD} = \begin{cases} \|\hat{a} - \hat{b}\|, & a \cdot b \geq 0 \\ \|\hat{a} + \hat{b}\|, & a \cdot b < 0. \end{cases} \quad (3.7)$$

The NAD between the normalized computed line changes and the normalized observed angle changes is computed for every line in the system. The line outage with the lowest NAD is the one with the lowest error and hence the predicted line outage. We note that the calculation above assumes that the system stays connected. It is possible that an line outage could island the system. The most common case occurs when a generator supplies the rest of the grid through a single line. If this line outages, then the generator bus forms one island and the rest of the grid forms the other island. Different calculations are needed for islanding cases as discussed in discussed in Section 3.3.2

### 3.3 Reduction to specified area

Tate and Overbye's method applies to the entire network. We now consider implementing the algorithm from the point of view of specified area of the system, where only that part of the system is observed. This fits the perspective of an entity such as a utility or balancing authority, which has control over only part of a larger system. The observable area must take into account the effects from other areas it connects to. Here we assume no knowledge of outside areas except measuring the power flows in the tie lines connecting

---

<sup>2</sup>This definition reformulates and simplifies the definition of [5] using the following result: For real vectors  $a$  and  $b$ , the sign of  $a \cdot b$  determines the minimum of  $\|a + b\|$  and  $\|a - b\|$ . Namely

$$\text{Min} \{\|a + b\|, \|a - b\|\} = \begin{cases} \|a - b\|, & a \cdot b \geq 0 \\ \|a + b\|, & a \cdot b < 0 \end{cases}$$

The result can easily be proved by noting that

$$\|a + b\|^2 - \|a - b\|^2 = (a + b) \cdot (a + b) - (a - b) \cdot (a - b) = 4a \cdot b$$

the outside areas to the observed area. In order to illustrate the method, we make the following simplifying assumptions

- only synchrophasor data from the area is available
- there was only one line outage
- power flows of all tie lines to the area are observable
- all of the area is connected (i.e. not multiple islands) before the outage

With these assumptions, we aim to model the area as if it was isolated from the rest of the network.

The DC load flow (3.1) gives a linear relationship between changes of angles and changes of power injections. Hence we can relate the changes in phasor angles using a superposition of the relevant power injections. The area's observed change in phasor angles after a line outage,  $\Delta\theta_{obs}$ , can be broken into two components:

$$\Delta\theta_{obs} = \Delta\theta_{area} + \Delta\theta_{into}. \quad (3.8)$$

Here  $\Delta\theta_{area}$  is the change in phasor angles due to system changes within the specified area assuming the area was isolated, and  $\Delta\theta_{into}$  is the change in phasor angles due to changes in power flow into the specified area through its tie lines.  $\Delta\theta_{obs}$  is obtained from the synchrophasor measurements observed before and after the outage.

Since we observe all tie line flows, we also have the change in power flows into the area. We view these changes as power injections at the border buses.  $P_{into}$  is the vector of power injections representing the tie line flows into the area, which is only non-zero at border buses. Following the structure of (3.1), we have

$$\Delta\theta_{into} = B^{-1}\Delta P_{into}. \quad (3.9)$$



Note that even if there is no generation redispatch and the net power flow into the area remains the same, a line outage will generally change the power flow distribution in the tie lines. These changes in power flows into the area will affect phasors throughout the area. In order to recognize the angle changes only due to the area's line outage,  $\Delta\theta_{into}$  is subtracted, leaving only the changes within the area

$$\Delta\theta_{area} = \Delta\theta_{obs} - \Delta\theta_{into}. \quad (3.10)$$

Removing the effects of the change in power flows into the area allows us to treat the observed area as an isolated area without need of information from inside the neighboring areas.

It is convenient to express all the angles relative to the same reference bus in the area, and the reference bus should be one of the area buses with phasor measurements. In reference-shifting, a constant value is added to the angles such that the reference bus is at zero. It follows that changes in angles at the reference bus are also zero, and that the corresponding component of all the vectors of angle changes in (3.10) will be zero.

The same basic steps are followed for all tested line outages, but there are differences in the calculations depending on whether the tested outage is non-islanding or islanding. Thus, we must first evaluate if a particular line outage would island the area. This is done by removing the line from the set of lines in the area and analyzing the buses that remain connected. Each set of connected buses is a separate island. If there is more than one such set of connected buses, that means the area has disconnected into separate islands after the line outage.

### 3.3.1 Non-islanding outage

We begin with non-islanding outages. As the system stays connected, there is no generation redispatch. The outaged line's removal from the system is the only change within the area itself. The angles change only due to removing the line, and we compute  $\Delta\theta_{outage}$  as

$$\Delta\theta_{outage} = \Delta\theta_{area} \quad (3.11)$$

where we know  $\Delta\theta_{area}$  from (3.10).

As discussed in section 3.2, the outages are modeled using equal and opposite power injections. Following (3.6),  $\Delta\tilde{\theta}_{calc,l}$  is

$$\Delta\tilde{\theta}_{calc,l} = KB^{-1} \begin{bmatrix} \mathbf{0} \\ 1 \\ \mathbf{0} \\ -1 \\ \mathbf{0} \end{bmatrix} \quad (3.12)$$

We define reference-shifting as

$$\bar{\theta} = \theta - \theta^{ref} \quad (3.13)$$

where  $\theta^{ref}$  is the value of the angle at the reference bus of vector  $\theta$ .

We express all angles with respect to the same reference bus which is one of the buses in the area with phasor measurements. After reference-shifting, the normalized vectors are used to compare the shape of the calculated angle change vector to that of the observed angle change vector.

We compare the reference-shifted, normalized angles to get the NAD for each line  $l$

in the area

$$\text{NAD}_l = \begin{cases} \|\Delta\hat{\theta}_{outage} - \Delta\hat{\theta}_{calc,l}\|, & \Delta\bar{\theta}_{outage} \cdot \Delta\bar{\theta}_{calc,l} \geq 0 \\ \|\Delta\hat{\theta}_{outage} + \Delta\hat{\theta}_{calc,l}\|, & \Delta\bar{\theta}_{outage} \cdot \Delta\bar{\theta}_{calc,l} < 0 \end{cases} \quad (3.14)$$

### 3.3.2 Islanding outage

Since the area is assumed to be initially connected, a single line outage islanding the area must produce exactly two islands,  $I_1$  and  $I_2$ . The islanding line must be the only line which connects  $I_1$  and  $I_2$ .

The method is more complicated when a line outage islands the area, and a different approach to modeling the line outage is needed. To accurately estimate the change in the bus phase angles in such a case, two factors must be taken into account

*Redispatch:* The islanding line outage generally results in an imbalance in generation and load in each island. If there is no load shed, the steady-state reached after the outage must have resolved these imbalances by generation redispatch.

*Island Referencing:* Due to the islanding, buses on the two islands can vary independently, but the bus phase angles are still related to each other within each island and a reference bus for each island is needed.

To estimate the correct angle relations for an islanding outage we determine the redispatch effects and then shift the angles according to each island's reference.

We note that the islanding considered here is islanding of the area considered separately from the entire network. When the area is islanded, it is possible that the entire network is islanded or that the entire network remains connected. If the entire network remains connected, the generation is not redispatched because the generation imbalance in the islands is supplied from the rest of the network through the area tie lines.

### Line outage modeling

The islanding case cannot model the line outage using the method of the connected case [8,9]. (Since the islanding line  $l$  must be the only line which connects the two areas, its power transfer distribution factor for the equal and opposite power injections at the ends of the line is  $PTDF_{l,l_{to}-l_{from}} = -1$  and the required power injection  $\tilde{P}_l$  in (3.5) becomes infinite.)

When the line outages, there are three components to the changes in the overall power balance in each island. First, there is the change in tie line flows,  $\Delta P_{into}$ , as previously discussed. Secondly, the outage of the line changes the overall island power balance by the amount of power flow on the line  $P_l$ , requiring a redispatch of that magnitude in each island. We refer to this portion of the redispatch as  $\Delta P_{outage}$ . Lastly, the change in the net power entering each island along the tie lines creates an additional imbalance requiring another component of generation redispatch,  $\Delta P_{in}$ . These three elements make up the power injections to model an islanding line outage in the subnetwork:

$$\Delta P = \Delta P_{into} + \Delta P_{outage} + \Delta P_{in}. \quad (3.15)$$

The rest of the subsection specifies  $\Delta P_{outage}$  and  $\Delta P_{in}$  in more detail.

We write  $\Delta p_1$  for the total change in the power entering island 1 and  $\Delta p_2$  for the total change in the power entering island 2; these are calculated by summing the power flows entering each island along tie lines:

$$\Delta p_I = \sum_{j \text{ in border of island } I} \Delta P_{into,j}, \quad I = 1, 2. \quad (3.16)$$

It is convenient in the explanation that follows to assume that the orientation of line  $l$  is chosen so that the “from” bus of line  $l$  is in area 2. Before the islanding outage, the islanding line has power flow  $P_l$  that is transferring power from area 2 to area 1. After

the line outage, there is a deficit of power  $P_l - \Delta p_1$  in area 1 and a surplus of power  $P_l + \Delta p_2$  in area 2. To reach steady state, there must be power redispatch in each area to restore balance. Let  $g_1$  be the total generation in island 1 and  $g_2$  the total generation in island 2. Then the required changes in total generation in each island are

$$\Delta g_1 = P_l - \Delta p_1 \tag{3.17}$$

$$\Delta g_2 = -P_l - \Delta p_2, \tag{3.18}$$

Implementing the generation redispatch will balance the power flow in each island. Moreover, in the network model of the area that includes the outaged line, the generator redispatch causes the line flow to be zero. And the powers entering the “to” bus of line  $l$  from the lines of island 1 sum to zero and the powers entering the “from” bus of line  $l$  from the lines of island 2 sum to zero. Thus the redispatch correctly models the effect of the islanding line outage *inside* each island. However, the islands are no longer synchronized, and differences between an angle in one island and an angle in the other island is not well defined. This problem is addressed below by choosing angle references in each island.

To implement the redispatch in each island, it is both necessary and part of the modeling to define the participation of the generators in each island. Any specific participation can be assumed, but here for definiteness we assume that the generators in each island participate in the redispatch in proportion to their generation. Then, recalling that the total generation in island  $I$  is  $g_I$ , the participation of each area bus in the redispatch is

given in the vector  $\gamma$ , where

$$(\gamma)_i = \begin{cases} (\text{generation at bus } i)/g_1, & \text{bus } i \text{ a generator in island 1} \\ -(\text{generation at bus } i)/g_2, & \text{bus } i \text{ a generator in island 2} \\ 0 & \text{otherwise} \end{cases} \quad (3.19)$$

Let  $\Delta\vec{g}$  be the vector with entries  $\Delta g_1$  corresponding to the buses of island 1 and  $-\Delta g_2$  corresponding to the buses of island 2.

$$(\Delta\vec{g})_i = \begin{cases} \Delta g_1, & \text{bus } i \text{ in island 1} \\ -\Delta g_2, & \text{bus } i \text{ in island 2} \end{cases} \quad (3.20)$$

It is now notationally convenient to reorder the buses so that the buses in island 1 come first. Then<sup>3</sup>

$$\Delta\vec{g} = \begin{pmatrix} \Delta g_1 \mathbf{1} \\ -\Delta g_2 \mathbf{1} \end{pmatrix} \quad (3.21)$$

and

$$\gamma = \begin{pmatrix} \gamma_1 \\ -\gamma_2 \end{pmatrix}. \quad (3.22)$$

Then the power injections that specify the redispatch in the area buses are  $\Delta P_{area}$  where

$$\Delta P_{area} = \begin{pmatrix} \Delta g_1 \gamma_1 \\ -\Delta g_2 \gamma_2 \end{pmatrix} = \Delta P_{in} + \Delta P_{outage} \quad (3.23)$$

---

<sup>3</sup> $\mathbf{1}$  is a column vector of all ones with the number of components chosen to fit the context.

where

$$\Delta P_{outage} = P_l \gamma \quad (3.24)$$

and

$$\Delta P_{in} = - \begin{pmatrix} \Delta p_1 \gamma_1 \\ \Delta p_2 \gamma_2 \end{pmatrix}. \quad (3.25)$$

### Redispatch

Now we turn to the actual algorithm to detect the line outage in this case, first addressing the redispatch aspect of the outage. We turn again to (3.8), reformulating it similarly to the division in (3.23)

$$\begin{aligned} \Delta \theta_{obs} &= \Delta \theta_{area} + \Delta \theta_{into} \\ &= \Delta \theta_{in} + \Delta \theta_{outage} + \Delta \theta_{into}. \end{aligned} \quad (3.26)$$

$\Delta \theta_{outage}$  is the change in area angles due to power imbalance directly caused by the line outage.  $\Delta \theta_{into}$  is known from the tie line power changes using (3.9).  $\Delta P_{in}$  is known by summing the tie line power changes to obtain  $\Delta p$ , and then  $\Delta \theta_{in} = KB^{-1} \Delta P_{in}$ . We rearrange (3.26) to express the desired angle change component in terms of the changes in angles that can be obtained from the measurements.

$$\begin{aligned} \Delta \theta_{outage} &= \Delta \theta_{obs} - \Delta \theta_{into} - \Delta \theta_{in} \\ &= \Delta \theta_{obs} - KB^{-1} (\Delta P_{into} + \Delta P_{in}) \end{aligned} \quad (3.27)$$

$\Delta \theta_{outage}$  is to be compared to the calculated results from the line topology.

We write  $\Delta P_{calc,l}$  for the calculated change in power injections directly caused by the

outage of line  $l$  so that  $\Delta P_{calc,l} = \Delta P_{outage}$  as given in (3.24). We use (3.24) to reformulate (3.6) for the islanding case

$$\Delta\theta_{calc,l} = KB^{-1}\Delta P_{calc,l} = P_l KB^{-1}\gamma_{calc,l} \quad (3.28)$$

which gives us

$$\Delta\tilde{\theta}_{calc,l} = KB^{-1}\gamma_{calc,l}. \quad (3.29)$$

### Island referencing

$\Delta\theta_{outage}$  and  $\Delta\tilde{\theta}_{calc,l}$  must now be appropriately reference-shifted to compare their shapes.  $\Delta\tilde{\theta}_{calc,l}$  cannot be used exactly the same way as the connected network case because the islands are decoupled. The phases of one island may shift with respect to the phases of the other island while maintaining their proper relation between phases within each island. Such shifts affect the normalization of overall system. To avoid any such shift between the observed angles and the calculated angles, we assign a reference bus for each island and express each angle in the area with respect to the reference bus angle for its island. We indicate the shifting of the angles with respect to the appropriate reference by an overbar:

$$(\bar{\theta})_i = \begin{cases} \theta_i - \theta_1^{\text{ref}}, & \text{bus } i \text{ in island 1} \\ \theta_i - \theta_2^{\text{ref}}, & \text{bus } i \text{ in island 2} \end{cases} \quad (3.30)$$

where  $\theta_I^{\text{ref}}$  is the reference bus angle of island  $I$ . The shifting of (3.30) is applied to  $\Delta\theta_{calc,l}$  and  $\Delta\theta_{outage}$ . Then the NAD of the outage of islanding line  $l$  can be calculated as

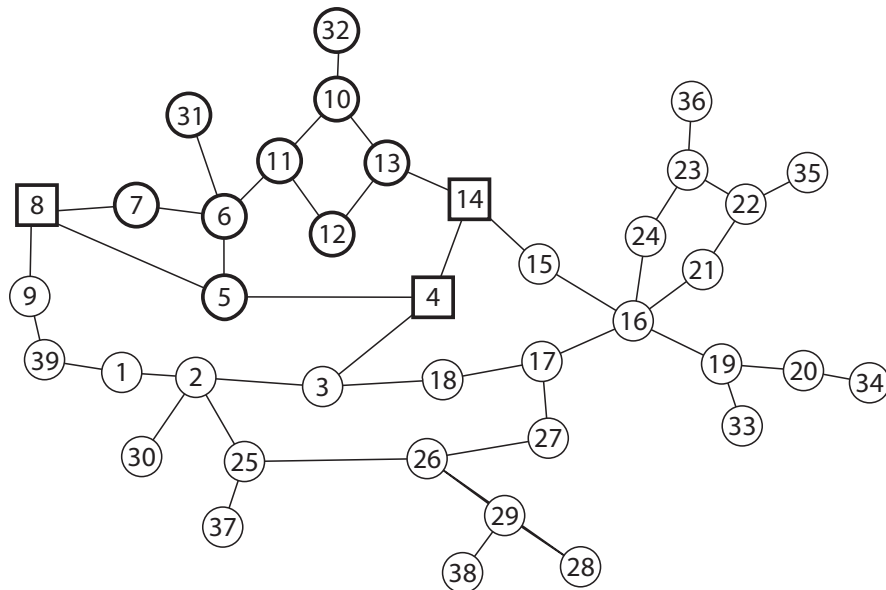
$$\text{NAD}_l = \begin{cases} \|\Delta\hat{\theta}_{outage} - \Delta\hat{\theta}_{calc,l}\|, & \Delta\bar{\theta}_{outage} \cdot \Delta\bar{\theta}_{calc,l} \geq 0 \\ \|\Delta\hat{\theta}_{outage} + \Delta\hat{\theta}_{calc,l}\|, & \Delta\bar{\theta}_{outage} \cdot \Delta\bar{\theta}_{calc,l} < 0 \end{cases} \quad (3.31)$$



### 3.3.3 Example

We test the implementation of the algorithm with computer calculations using Mathematica. A reduced New England system DC load flow model with 39 buses is used as illustrated in Fig. 3.1. The bolded area in the figure is selected for study due to the different categories of line outages available within the area. We illustrate the dependency of the algorithm on the synchrophasor bus selection by fixing the number of synchrophasors in the area to 5 and comparing the results of two selections of sets of 5 synchrophasors.

Figure 3.1: Reduced New England System Model



The results of the algorithm in simulations of all 14 possible line outages within the area are listed in Table 3.1. For synchrophasor Set 1, we have synchrophasors at buses 4, 8, 14, 31, and 32. With this synchrophasor set, the algorithm specified the exact line outage for every line except lines 6-7, 7-8, 12-11, and 12-13. With synchrophasor Set 2 that has synchrophasors at 4, 8, 14, 12, and 32, we have the same results as the synchrophasor Set 1 except that the ambiguities for the outage of lines 12-11 and 12-13 disappear, while gaining an ambiguity for the outage of 31-6.

Table 3.1: Predicted Outage According to synchrophasor Buses

<b>Outage</b>	synchrophasor Bus Set 1:	synchrophasor Bus Set 2:
	4, 8, 14, 31, 32	4, 8, 14, 12, 32
4-5	4-5	4-5
4-14	4-14	4-14
5-6	5-6	5-6
5-8	5-8	5-8
6-7	6-7, 7-8	6-7, 7-8
6-11	6-11	6-11
7-8	6-7, 7-8	6-7, 7-8
10-11	10-11	10-11
10-13	10-13	10-13
13-14	13-14	13-14
31-6	31-6	31-6, 10-32
10-32	10-32	10-32
12-11	12-11, 12-13	12-11
12-13	12-11, 12-13	12-13

To explain the ambiguities, we begin by focusing on the difference between the results of the synchrophasor sets. By simply moving a synchrophasor from bus 31 to bus 12, we remove ambiguity from two line outage cases and added an ambiguity to one line outage case. For the observed area, there are only two generator buses, 31 and 32, and they are both at the end of radial lines. The outage of one the radial lines will island generation, necessitating the redispatch of the other. From the point of view of the rest of the system, the loss of one of these radial lines will be a power loss where it connected to the rest of the system, but there will also be a power injection at the connection of the other radial line due to the redispatch of the other generator to make up for the power loss.

The outage of a radial line will cause the bus at the end of it to become a disconnected island with one isolated bus. Only the differences in phasor angles between buses in an island have value, hence a lone phasor angle gives no information about that island and we can detect no error from it. However, if we have a synchrophasor at the other radial

line's bus, we can detect the error from the redispatch as it will generally not fit the redispatch if it were disconnected from the system. This is why synchrophasor Set 2, which has no synchrophasor at bus 31, cannot detect the error from the outage of line 31-6.

The ambiguity between lines 12-11 and 12-13 for synchrophasor Set 1 is due to the lines being in series. Viewing a line outage as a pair of equal and opposite power injections at the ends of the line, we see that a line outage of either 12-11 or 12-13 will be a pair of such power injections between the series pair of lines between buses 11 and 13. From the point of view of the system outside the two lines, these power injections will be equivalent to power injections at the ends of the two lines at buses 11 and 13. This is because the pair of lines has a set load which is balanced before the outage with a certain power flow from outside the pair of lines. After the pair of injections are added, the system outside the pair of lines is still balanced with the same flows as before, but is now superimposed on the flows from the added pair of injections from the two lines in series.

The magnitude of the power injections may differ depending on the line, but because they are equal and opposite, they have proportional effects from the point of view of the system outside the pair of lines. Hence, synchrophasor Set 1 cannot distinguish between the outage of line 12-11 and the outage of line 12-13. On the other hand, synchrophasor Set 2 has a synchrophasor at bus 12 within the series of lines, which allows the algorithm to distinguish the change in angles within the pair of lines. Note that the ambiguity of lines 6-7 and 7-8 is of the same type.

### 3.4 Conclusions

It is often convenient and pragmatic to work with models and measurements within a specific power system area inside a larger grid interconnection. We have shown how synchrophasor measurements of voltage and current around the border of an area can be

used together with synchrophasor voltage measurements inside the area and a DC load flow model of the area to detect single line outages in the area and discriminate which line outaged. The method extends Tate and Overbye's method of line outage identification [5] to apply to a specific area.

We also give a way to model the effect of line outages that island the area, since the usual modeling of line outages by power injections at the ends of the line does not work for the islanding case. Hence we are able to also discriminate these islanding line outages with synchrophasor measurements.

## Chapter 4

### Examples of voltages across areas in WECC

After briefly overviewing the concept of a voltage angle across an area of a power system, we illustrate defining voltage angles across several areas of WECC using a DC load flow WECC model. The voltage angle across an area indicates the stress on an area. One of the examples shows the stress measured by the voltage angle across an area increasing as some of the events of the September 2011 San Diego blackout occur. The remaining examples focus on areas concerning the California-Oregon Intertie.

#### 4.0.1 Angle across an area

The concept of the voltage angle across a power system area is new and is described in detail in [3]. Here we give a brief overview of the voltage angle across an area.

In a DC load flow of an area of a power system, the voltage phasor angle across an area can be defined by suitably combining voltage angles at buses on the border of the area. For example, to get the angle difference north-south across an area, a weighted combination of angles at buses on the southern tie lines are subtracted from a weighted combination of angles at buses on the northern tie lines.<sup>1</sup>

The angle across an area is a generalization of the angle difference at two buses. The angle across an area is useful because it summarizes the circuit behavior of the area. In particular, the angle across the area satisfies the basic circuit law so that the effective power flow through the area is the product of the angle across the area and the effective susceptance of the area.

The angle across an area seems promising for power system monitoring, and here

---

<sup>1</sup>Note that when defining the angle across the area, it is required to include all ties lines all the way around the border of the area (otherwise power flows can “escape” without being tracked), so the tie lines must all be grouped into one of the two “sides” of the area.

we are most interested in their application to quantify stress across an area. The stress interpretation of the area angle works in the same way that the angle across a single transmission line indicates the transmission line stress. It is hypothesized that the limits on area angles may usefully capture in a bulk measure some of the salient limits within the area.

Unlike the angle difference at two buses, which is related to power flows in all parts of the network, the angle across an area describes the stress that the particular area is experiencing due to power flows both inside and through the area. Indeed the total angle across the area  $\hat{\theta}_{ab}$  can be decomposed into an “internal” angle  $\hat{\theta}_{ab}^R$  due to generation and load inside the area and an “external” angle  $\hat{\theta}_{ab}^{into}$  that is due to power flow through the area from the rest of the power system.

$$\hat{\theta}_{ab} = \hat{\theta}_{ab}^R + \hat{\theta}_{ab}^{into} \quad (4.1)$$

The internal angle  $\hat{\theta}_{ab}^{into}$  is useful because it only responds to changes inside the area. The presence or absence of changes in  $\hat{\theta}_{ab}^{into}$  discriminates whether events occur inside or outside the area.

## 4.0.2 Simple example

Fig. 4.1 shows a simple example of a power system area with border buses 31,32,39,4,14. The rest of the network is not shown in Fig. 4.1. We define the angle  $\hat{\theta}_{ab}$  across the area from buses 31, 32 to buses 39,4,14. In the base case for this power system,  $\hat{\theta}_{ab} = 10.07$  degrees, the power flow through the area is  $P_{ab} = 9.825$  pu and the area equivalent susceptance is  $b_{ab} = 55.88$  pu.

In this case, the angle across the area is calculated as the following weighted combi-

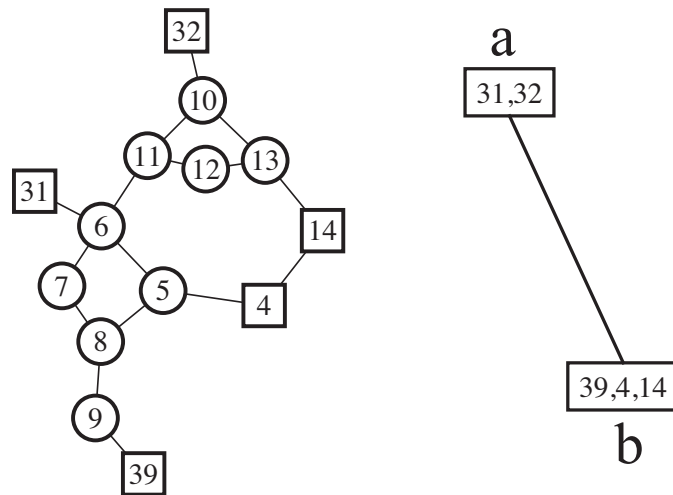


Figure 4.1: A power system area to show the angle across the area from buses 31, 32 to buses 39,4,14. The area angle can be thought of as the angle across the single transmission line a-b shown that is a reduced equivalent of the area.

nation of the angles at the border buses:

$$\hat{\theta}_{ab} = 0.4587\theta_{31} + 0.5413\theta_{32} - 0.0863\theta_{39} - 0.4167\theta_4 - 0.4970\theta_{14} \quad (4.2)$$

The angle across the area can be easily computed from synchrophasor measurements of the voltages at the border buses of the area.

## 4.1 Southern California area

### 4.1.1 Methodology overview

This section discusses using area angles for the analysis of events on the WECC system which parallels some of the major events leading up to the San Diego area blackout of September 2011. The calculations were done using Mathematica on a DC load flow model of WECC with 1,553 buses and 2,114 lines as shown in Fig. 4.2. Note that Fig. 4.2 is drawn automatically based only on the topological structure of the WECC model and does not follow exact geographic relations, though there may be some rough

correspondence of areas of the figure with geographic locations. A few buses are labeled to give a sense of location for parts of the system that are relatively near.

We examine the impact of three major events that occurred during the progression of the cascading failure that lead to the blackout. In chronological order, the events are 1) the trip of the 500 kV Hassayampa-North Gila line, 2) the loss of 420 MW from La Rosita unit trips (modeled with a redispatch at Rinaldi to keep balance), and 3) the trip of the San Onofre Nuclear Generating Station (SONGS). Due to the compounding effects of the events on the structure of the system, we cannot analyze the effects of each event separately. Thus we look at the four cases

1. Prior the events (normal state)
2. After Hassayampa-North Gila trip
3. After La Rosita generation loss
4. After SONGS trip

The events accumulate as the cases progress. For example, after the La Rosita generation loss the system has both the Hassayampa-North Gila line outaged and the La Rosita generation loss.

The system stress is analyzed using area angles as the events occur. Four different areas are chosen based on the structure of the southern California system and different aspects of the system are observed.

The four areas are chosen to measure the following stresses:

1. The east-west stress between SONGS and Imperial Valley
2. Stress from SONGS to major generation towards the east side of the southern California area





Figure 4.2: WECC model

3. The north-south stress from SONGS and Imperial Valley to buses of major load in Mexico
4. Stress funneling through SONGS from North Los Angeles down through SONGS to Imperial Valley

Each area is defined by two groups of buses, one group on each “side” of the area, which are referred to as the area’s “border” sets, though the buses need not all be on the borders of the area. We refer to these border sets as M1 and M2, and the area angle is the angle across the area from M1 to M2. The four areas are defined with the following bus sets:

1. **M1:** SONGS  
**M2:** Imperial Valley
2. **M1:** SONGS  
**M2:** Imperial Valley, Mexicali, La Rosita, CTY, CPT, CPD
3. **M1:** SONGS, Imperial Valley  
**M2:** MEP, RUB, CIP, Tijuana, Mexicali, CPD, CTY, CRO
4. **M1:** Vincent, Lugo, Victorville, Adelanto, Devers, Mirage  
**M2:** Imperial Valley

The four areas and their border sets are shown in Figure 4.3. The buses in the border sets are indicated by the arrows, with black arrows for M1 and white arrows for M2.

### 4.1.2 Results

The area angle of each of the four areas is calculated after each of the four events. An exception is that the Area 4 angle after event 4 cannot be calculated because the area angle cannot be applied to an area containing disconnected parts [3]. The results display

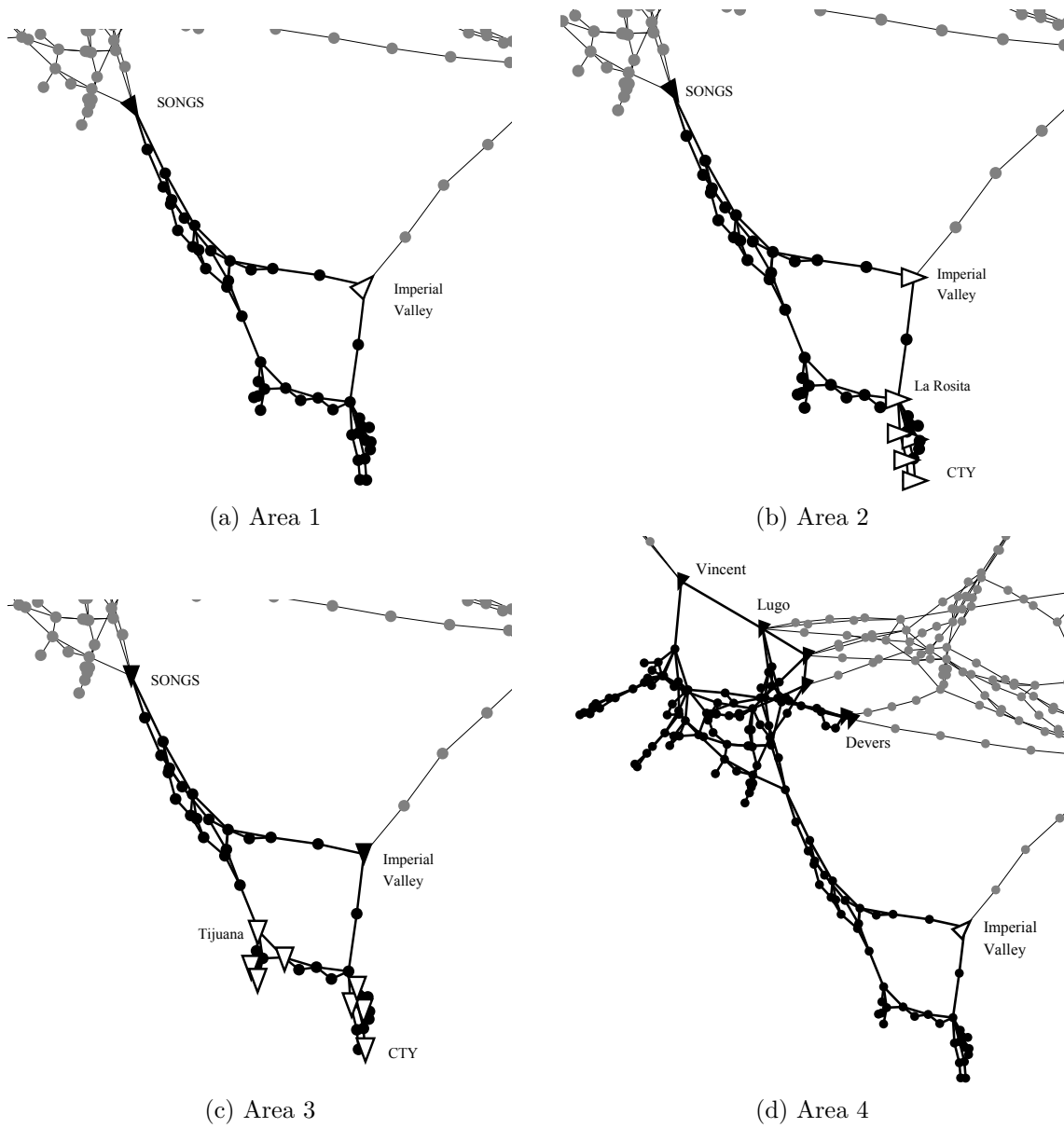


Figure 4.3: Southern California areas. Area border buses are shown as triangles.

the total area angle  $\hat{\theta}_A$  and its two components, the external angle  $\hat{\theta}_A^{into}$  and internal angle  $\hat{\theta}_A^R$ . The formulas for computing these area angles are given in [3].

Two subtables are shown for each area in Tables 4.1–4.4. Subtable (a) lists the angles after each of the 4 events and Subtable (b) shows the change in angles after each event.

Table 4.1: Area 1 (in degrees)

(a) Angle Values				
	1. Before	2. Trip N.Gila-Hassa.	3. Trip LaRosita	4. Trip SONGS
$\hat{\theta}_{A1}$	-13.06	11.10	18.44	-28.93
$\hat{\theta}_{A1}^{into}$	-23.41	0.7563	4.712	7.370
$\hat{\theta}_{A1}^R$	10.35	10.34	13.73	-36.30

(b) Angle Changes			
	1. →2.	2. →3.	3. →4.
$\Delta\hat{\theta}_{A1}$	24.16	7.345	-47.38
$\Delta\hat{\theta}_{A1}^{into}$	24.17	3.956	2.657
$\Delta\hat{\theta}_{A1}^R$	-0.005901	3.389	-50.03

Table 4.2: Area 2 (in degrees)

(a) Angle Values				
	1. Before	2. Trip N.Gila-Hassa.	3. Trip LaRosita	4. Trip SONGS
$\hat{\theta}_{A2}$	-12.82	11.09	18.94	-29.37
$\hat{\theta}_{A2}^{into}$	-23.15	0.7478	4.660	7.345
$\hat{\theta}_{A2}^R$	10.33	10.35	14.28	-36.72

(b) Angle Changes			
	1. →2.	2. →3.	3. →4.
$\Delta\hat{\theta}_{A2}$	23.91	7.845	-48.31
$\Delta\hat{\theta}_{A2}^{into}$	23.90	3.912	2.685
$\Delta\hat{\theta}_{A2}^R$	0.01125	3.933	-50.99

Beginning with Area 1, we notice that each event causes significant changes to the area angle  $\hat{\theta}_A$ , but the change is extremely large after the islanding when SONGS trips, indicating a tremendous change in the east-west stress between SONGS and Imperial

Table 4.3: Area 3 (in degrees)

(a) Angle Values

	1. Before	2. Trip N.Gila-Hassa.	3. Trip LaRosita	4. Trip SONGS
$\hat{\theta}_{A3}$	5.116	5.116	6.890	0.7862
$\hat{\theta}_{A3}^{\text{into}}$	-1.116	-1.116	0.06437	-0.7459
$\hat{\theta}_{A3}^{\text{R}}$	6.232	6.232	6.826	1.532

(b) Angle Changes

	1.→2.	2.→3.	3.→4.
$\Delta\hat{\theta}_{A3}$	0	1.774	-6.104
$\Delta\hat{\theta}_{A3}^{\text{into}}$	0	1.181	-0.8103
$\Delta\hat{\theta}_{A3}^{\text{R}}$	0	0.5936	-5.294

Table 4.4: Area 4 (in degrees)

(a) Angle Values

	1. Before	2. Trip N.Gila-Hassayampa	3. Trip LaRosita
$\hat{\theta}_{A4}$	-5.275	31.24	42.51
$\hat{\theta}_{A4}^{\text{into}}$	110.9	147.4	147.3
$\hat{\theta}_{A4}^{\text{R}}$	-116.2	-116.1	-104.8

(b) Angle Changes

	1.→2.	2.→3.
$\Delta\hat{\theta}_{A4}$	36.52	11.27
$\Delta\hat{\theta}_{A4}^{\text{into}}$	36.42	0
$\Delta\hat{\theta}_{A4}^{\text{R}}$	0.09124	11.27

Valley. In Area 2, the change in angles mirror those of Area 1 after the first and second events. The final event has somewhat different components of the angle, but they sum up to give a total change in area angle that is very similar to that of Area 1.

Area 2 is also an east-west area angle and though it includes additional buses from the South, the area angle change is the same as Area 1. Area 3 gives no change for the first event. The other two events are similar to the previous two, but with significantly smaller angle change magnitudes. All three areas seem to indicate an increase in the stress in one direction followed by a much bigger reversal after SONGS trips.

The area angle patterns of Areas 1-3 indicate an east-west oriented stress in the areas surrounding San Diego. The addition of buses in Mexico to the eastern border of Area 1 to form Area 2 had essentially no effect on the overall angle. The contributions of the more southern buses in Mexico seem to have been far outweighed by the components between SONGS and Imperial Valley so that the overall angle remained about the same. Area 3 showed no change for the trip of the N.Gila-Hassayampa line and smaller angle change magnitudes than Areas 1 and 2. The smaller sensitivity of Area 3 indicates that the events have a much smaller effect on the north-south stress of the system than on the east-west stress of the system.

Area 4 is larger than Areas 1, 2 and 3. It includes not only San Diego and North Baja, but also Los Angeles. The idea behind Area 4's definition is to include the stress north of SONGS. Though the northern border is defined very differently from the other area, Area 4's angle changes follow a pattern similar to those of Areas 1, 2 and 3 except with larger magnitudes. This indicates the stress through the SONGS area of the network was heavily influenced by the events.

Table 4.5: Percent Changes in  $\hat{\theta}_A$

Area	1. $\rightarrow$ 2.	2. $\rightarrow$ 3.
1	185.0	66.18
2	186.6	70.72
3	0	34.69
4	692.3	36.07

The change in values may be less significant for area angles that are larger i. e. the angle changes may be relatively small compared to the base angle value. To ascertain whether the angle changes are significant, we look at the magnitude of percent change of the area angles for the trip of the N.Gila-Hassayampa line and the loss of generation at La Rosita. We see in Table 4.5 that the patterns are similar to the those of the magnitude of angle change, except that the La Rosita trip is more sensitive to Areas 1 and 2 than

Area 4. This may be due to the fact that the La Rosita generation loss was made up at Rinaldi, which is included within Area 4 but outside the other areas.

## 4.2 Areas North and South of COI

We consider defining areas to analyze the areas related to the California-Oregon Intertie (COI). After defining areas north and south of the COI, we compute the angles across these areas for the base case and with a contingency condition. Setting up these areas in the fairly detailed WECC model<sup>2</sup> will be very useful in further work applying the area angles.

### 4.2.1 Area North of COI

The northern area is roughly the power transmission grid within the Washington and Oregon state borders. The north/east border (Border A) is made up of Custer W., Boundary, Lancaster, Rathdrum, Benewah, Benewah-Taft, Dworshak-Taft, Brownlee, Burns-Midpoint, and Hiltop buses. The south border (Border B) is made up of Captain Jack and Malin buses. The different borders are indicated with separate colors in the the electrical network in Figure 4.4.

The weights of the angles of each border bus used to compute the area angle are given in Table 4.6. In the base case, the area angle from Border A to Border B and its internal and external components are

$$\begin{aligned}\hat{\theta}_{ab} &= 36.4^\circ \\ \hat{\theta}_{ab}^{into} &= 24.2^\circ \\ \hat{\theta}_{ab}^R &= 12.3^\circ\end{aligned}$$

With the outage of line between Summer L. and Burns-Summer 1, the area stress

---

<sup>2</sup>One detail is that the sign of the susceptance for a section of the Dworshak-Taft line of this model was changed from negative to positive. Negative line susceptances can lead to bus weights of sign opposite to those expected in the formula for the area angle. A negative susceptance is non-physical, but arises in the model reduction process that was used to obtain the 1553 bus model. A more detailed WECC model would have positive susceptances for all lines.



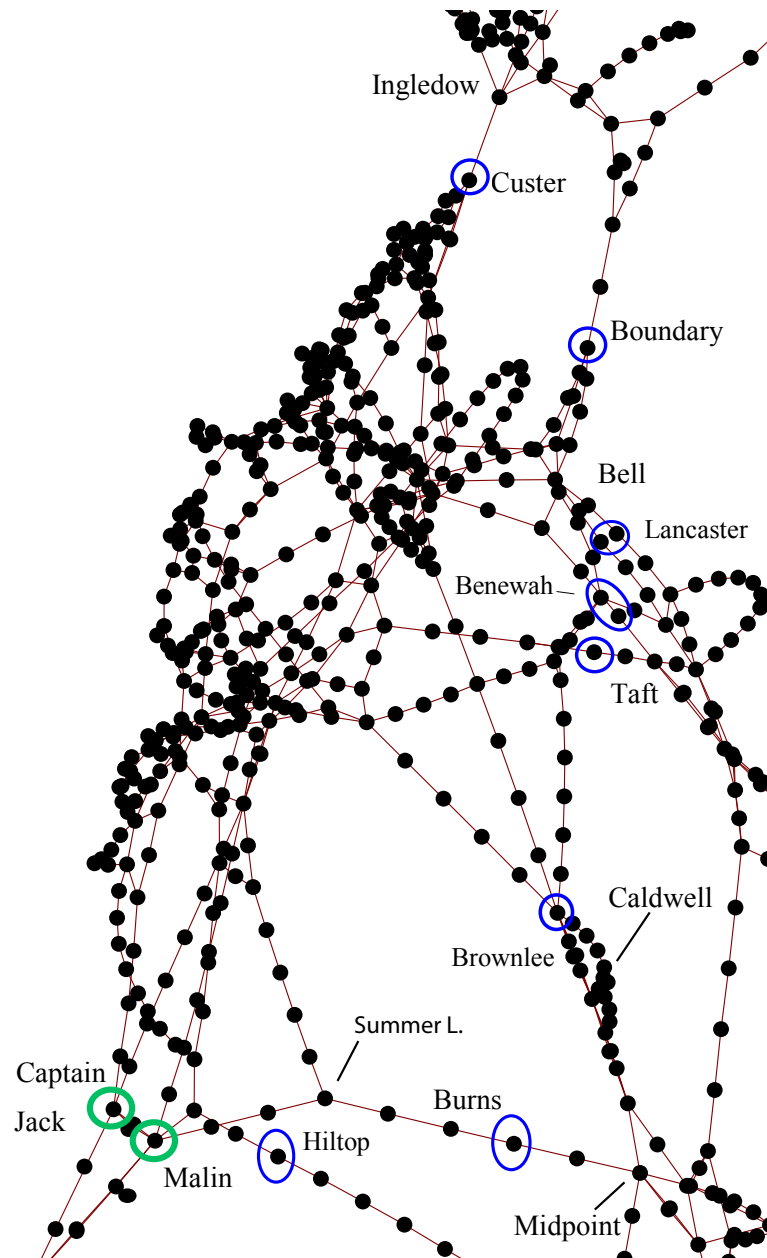


Figure 4.4: North of COI area electric network

Table 4.6: Border bus weighting in North of COI area angle

	<b>Border Bus Name</b>	<b>Weight</b>
Border A	Hiltop	0.124
	Burns-Midpoint 1	0.220
	Brownlee	0.055
	Dworshak-Taft 1	0.129
	Benewah	0.036
	Benewah-Taft 1	0.185
	Rathdrum	0.010
	Lancaster	0.008
	Boundary	0.006
	Custer W.	0.227
Border B	Captain Jack	-0.362
	Malin	-0.638

increases and the area angles become

$$\hat{\theta}_{ab,out} = 45.6^\circ$$

$$\hat{\theta}_{ab,out}^{into} = 30.2^\circ$$

$$\hat{\theta}_{ab,out}^R = 15.4^\circ$$

The positive area angle indicates a stress from the area's northeastern border to its southern border. This is what we would predict due to the large amount of generation of Canada and light load in the northeastern part of the area versus the large load towards the Bay Area. Also, the loss of the line increases the area stress as expected.

The positive external angle is positive due to the power flowing into the northern border from Canada's generation and power flowing out of the southern border to the Bay Area load. The positive internal angle may be largely due to the major loads of Seattle to Portland being so far from the area's eastern border. The internal angle is expected to be reduced due to Seattle's proximity to the northern border, but nearly all the border buses are on the eastern edge as clear from Figure 4.4.

## 4.2.2 Area South of COI

The southern area is roughly California from the Oregon border down to just north of the Los Angeles area. The northern border (Border A) is made up of buses Captain Jack and Malin. The area's southern border (Border B) made up of buses Midway-Vincent 2a, Midway-Vincent 2b, Midway-Vincent 3. The different borders are indicated with separate colors in the electrical network in Figure 4.5.

Table 4.7: Border bus weighting in South of COI area angle

	<b>Border Bus Name</b>	<b>Weight</b>
Border A	Captain Jack	0.345
	Malin	0.654
Border B	Midway-Vincent 2a	-0.322
	Midway-Vincent 2b	-0.322
	Vincent	-0.354

The weights of the angles of each border bus used to compute the area angle are given in Table 4.7. In the base case, the area angle from Border A to Border B and its internal and external components are

$$\begin{aligned}\hat{\theta}_{ab} &= 34.8^\circ \\ \hat{\theta}_{ab}^{into} &= 52.7^\circ \\ \hat{\theta}_{ab}^R &= -17.9^\circ\end{aligned}$$

With the outage of line between Midway and Midway-Vincent 1, the area stress

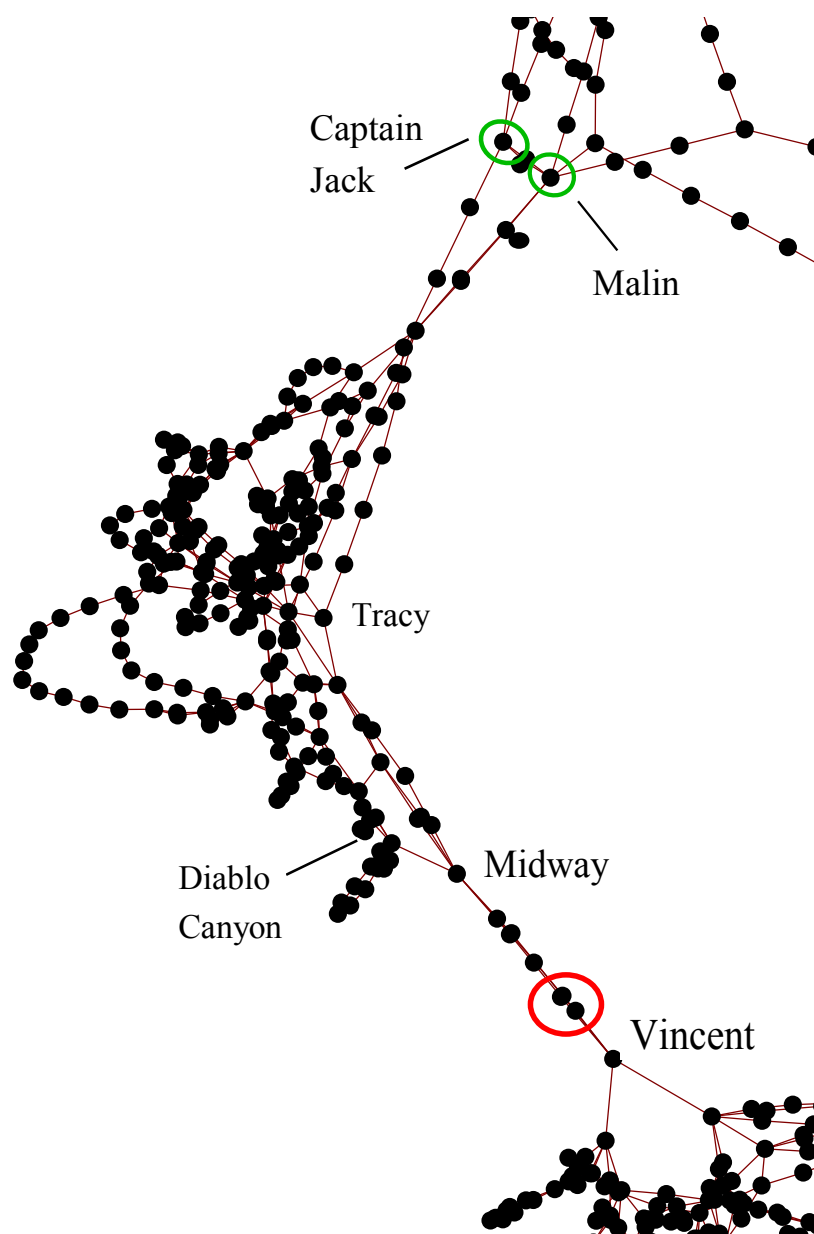


Figure 4.5: South of COI area electric network

increases and the area angles become

$$\begin{aligned}\hat{\theta}_{ab,out} &= 40.7^\circ \\ \hat{\theta}_{ab,out}^{into} &= 59.1^\circ \\ \hat{\theta}_{ab,out}^R &= -18.4^\circ\end{aligned}$$

The area's angle indicates a north-south stress. This makes intuitive sense as Northern California's hydro generation adds to the large powerflow entering from the northern border. The power is expected to flow down towards the Bay Area load. Generation south of the Bay Area, mainly at the nuclear plant Diablo Canyon can contribute to supplying both the Bay Area and Los Angeles loads. Just as in the area north of the COI, the line loss increases the area's stress as predicted.

The external angle is easily understood based on the powerflow from the generation from the north coming in through Northern California power lines as well as the powerflow leaving the area's southern border to supply Los Angeles. For the internal angle, we recognize that the major load of the Bay Area is towards the center of the area and would not be thought to favor either border, in and of itself. Most of the hydro is towards the northern portion of the area, but hydro generation is small compared that of the nuclear plant. Diablo Canyon is anticipated to send power towards Los Angeles but it seems that its component supplying the Bay Area dominates the internal angle.

## Bibliography

- [1] A.G. Phadke and J.S. Thorp, *Synchronized Phasor Measurements and Their Applications*. New York: Springer, 2008.
- [2] V. Venkatasubramanian, Y. X. Yue, G. Liu, M. Sherwood, and Q. Zhang, “Wide-area monitoring and control algorithms for large power systems using synchrophasors,” in *IEEE Power Systems Conference and Exposition*, Seattle, WA, March 2009.
- [3] I. Dobson, “Voltages across an area of a network,” in *IEEE Transactions on Power Systems*, May 2012, pp. 993–1002.
- [4] C. W. Taylor, D. C. Erickson, K. E. Martin, R. E. Wilson, and V. Venkatasubramanian, “WACS-wide-area stability and voltage control system: R&D and online demonstration,” in *Proceedings of the IEEE*, vol. 93, no. 5, May 2005, pp. 892–906.
- [5] J.E. Tate and T.J. Overbye, “Line outage detection using phasor angle measurements,” in *IEEE Transactions on Power Systems*, vol. 23, no. 4, November 2008, pp. 1644–1652.
- [6] A. Wood and B. Wollenberg, *Power Generation, Operation, and Control*. New York: Wiley, 1984.
- [7] M. Li, Q. Zhao, P.B. Luh, “DC power flow and its feasibility in systems with dynamic topology,” in *IEEE Power and Energy Society General Meeting*, Pittsburgh, PA, July 2008.
- [8] C. Davis, “Multiple-element contingency screening,” Ph.D. dissertation, University of Illinois at Urbana-Champaign, 2009.

- [9] T. Guler and G. Gross, "Detection of island formation and identification of causal factors under multiple line outages," in *IEEE Transactions on Power Systems*, vol. 22, no. 2, May 2007.